Picosecond Transient Photoconductivity in Functionalized Pentacene Molecular Crystals Probed by Terahertz Pulse Spectroscopy

F. A. Hegmann,[1,*] R. R. Tykwinski,[2] K. P. H. Lui,[1] J. E. Bullock,[3] and J. E. Anthony[3]
[1]*Department of Physics, University of Alberta, Edmonton, Alberta, Canada T6G 2J1*
[2]*Department of Chemistry, University of Alberta, Edmonton, Alberta, Canada T6G 2G2*
[3]*Department of Chemistry, University of Kentucky, Lexington, Kentucky 40506-0055*
(Received 11 July 2002; published 11 November 2002)

We have measured transient photoconductivity in functionalized pentacene molecular crystals using ultrafast optical pump–terahertz probe techniques. The single crystal samples were excited using 800 nm, 100 fs pulses, and the change in transmission of time-delayed, subpicosecond terahertz pulses was used to probe the photoconducting state over a temperature range from 10 to 300 K. A subpicosecond rise in photoconductivity is observed, suggesting that mobile carriers are a primary photoexcitation. At times longer than 4 ps, a power-law decay is observed consistent with dispersive transport.

DOI: 10.1103/PhysRevLett.89.227403 PACS numbers: 78.47.+p, 72.20.–i, 72.40.+w, 72.80.Le

Organic semiconductors show great promise for applications in electronics and photonics [1–4]. However, the nature of charge transport and primary photoexcitations in conjugated polymers [5] and organic molecular crystals [6–8] is not completely understood.

Conducting polymers such as doped polyacetylene have conductivities at room temperature close to that of copper [9,10]. However, unlike normal metals, the conductivity of doped polymers typically decreases as the temperature is lowered as described by variable-range hopping in disordered materials [10]. Furthermore, charge transport along polymer chains is in the form of polarons, bipolarons, and solitons [9,11]. Many organic semiconductors [12,13], as well as inorganic semiconductors such as amorphous silicon [14], exhibit dispersive transport due to disorder [15]. Dispersive transport can be identified in time-of-flight experiments as a transient photocurrent that varies as $t^{\alpha-1}$ for times less than the transit time, where α is called the dispersion parameter [15]. The mobility, μ, for polymer films is typically less than 10^{-2} cm^2/V s at room temperature [13]. Typical mobilities for holes injected at room temperature into ultrapure polyacene single crystals such as naphthalene (Nph) and pentacene (Pc) are around 1 cm^2/V s [16,17]. However, the temperature dependence of the mobility in these crystals varies as $\mu \sim T^{-n}$ ($n \sim 1.4$ to 2.9), similar to bandlike transport seen in inorganic semiconductors [18]. At low temperatures ($T < 30$ K), the carrier mobility levels off at values greater than 100 cm^2/V s for Nph [16] and 10^4 cm^2/V s for Pc [17]. At higher temperatures, a transition from band transport to hopping transport is observed in Nph [19], Pc, and other organic molecular crystals [20] consistent with some polaron models [7,8,20]. However, questions still remain regarding the nature of charge transport in organic molecular crystals [21].

There is also debate over the nature of primary photoexcitations in conjugated polymers [5]. In the molecular exciton model, the primary photoexcitations are excitons which can be dissociated by electric fields or other mechanisms into separated polarons, as shown by several groups using ultrafast pump-probe techniques on polymer thin films [22,23]. On the other hand, the semiconductor band model claims that mobile polarons are created directly by the absorption of light, as demonstrated by transient photoconductivity and ultrafast pump-probe experiments on polymer thin films [24,25]. Frenkel excitons are believed to be the primary photoexcitations in organic molecular crystals [26]. Exciton dynamics in α-hexathiophene [26] and tetracene [27] single crystals have been recently studied using ultrafast pump-probe techniques, but these experiments are not sensitive to carrier transport. Transient photoconductivity has been measured in pentacene [7] and α-octithiophene [28] single crystals with 10 ns and 25 ps time resolution, respectively, but noncontact techniques with better time resolution are desirable.

In this Letter, we report the first optical pump-terahertz probe measurements of transient carrier dynamics in an organic molecular crystal. Terahertz time-domain spectroscopy (THz-TDS) has become a powerful technique for studying the conductivity of materials in the far-infrared region of the spectrum [29–32]. Furthermore, the subpicosecond duration of THz pulses is ideal for noncontact measurements of transient conductivity in materials. For instance, optical pump–THz probe techniques have been used to study carrier dynamics in GaAs [33,34], LT-GaAs [35], silicon-on-sapphire [36], and manganites [37]. THz pulse spectroscopy has also been used to study the dynamics of solvated electrons in liquids [38] and intramolecular charge transfer in dye solutions [39]. A key advantage of THz pulses is their sensitivity to the conductivity of a material. Therefore, THz pulse spectroscopy should provide further insight into the nature of carrier dynamics in organic materials.

The molecular structure of the functionalized pentacene (FPc) derivative [40] used in these experiments is shown in Fig. 1(a). The triisopropylsilylethynyl side groups increase the solubility of the pentacene molecule making it easier to grow single crystals from solution. Furthermore, the side groups force the pentacene molecules to stack like bricks in a wall [40], as shown in Fig. 1(b), rather than in the herringbone structure of pristine Pc crystals, resulting in enhanced intermolecular π-orbital overlap in FPc crystals. Samples were initially purified by recrystallization from a tetrahydrofuran (THF) solution via the addition of methanol. Large, single crystals were then grown via vapor diffusion of methanol into a saturated THF solution at 4 °C. The diffusion process at this temperature takes approximately 4 to 5 days to reach completion. The single crystal samples were typically 2 mm $\times$ 4 mm with a thickness of about 0.5 mm, and were mounted on a 1-mm-diameter aperture inside an optical cryostat (sample in vapor). Several FPc samples were used in these experiments, but only the results from two crystals (samples A and B) are presented here.

As described elsewhere [36], a 100 fs, 800 nm, 1 kHz, amplified Ti:sapphire laser source was used to generate THz pulses via optical rectification in a 0.5-mm-thick ZnTe crystal. The electric field of the THz pulse was detected by free-space electro-optic sampling in a 2-mm-thick ZnTe crystal. The transmission of the THz pulse through the sample was monitored as a function of delay time with respect to an 800 nm, 100 fs pump pulse. Both the THz probe and 800 nm pump pulses were at normal incidence to the face of the FPc crystal. The electric field of the THz pulse was, therefore, in the *a-b* plane [Fig. 1(b)], but polarized predominantly along the π-stacking direction. The pump pulse is close to an absorption edge near 800 nm in the FPc crystal, and the optical penetration depth is about 120 μm resulting in bulk excitation of the sample. The origin of this absorption edge is not known at this time, but it appears only in the solid-state form of FPc and not in isolated FPc molecules in solution. Also, earlier measurements on FPc crystals revealed a maximum photoresponse centered around 800 nm (1.55 eV) [41]. For comparison, the onset of photoconduction in Pc crystals occurs at 550 nm (2.25 eV) [7]. Incident pump fluences of about 2.5 mJ/cm^2 ($\sim$ 20 μJ per pulse in a 1-mm-diameter aperture) produced carrier densities from 10^{17} to 10^{18} cm^{-3}. Figure 2(a) shows examples of THz pulses transmitted through a FPc sample at 10 K for various delay times with respect to the pump pulse. The inset of Fig. 2(a) shows the corresponding amplitude spectrum of the THz pulse transmitted through the unexcited sample. No absorption lines due to phonons in the FPc samples were observed in this frequency range. (The spectrum is narrower than usual due to spatial filtering of low frequency components by the 1-mm-diameter aperture and attenuation of higher frequency components by the glass windows of the cryostat.) The transmitted amplitude of the THz pulse is reduced by the presence of photoexcited carriers in the sample, but no phase shift is observed. This implies that $\omega\tau < 1$ for our measurements, where τ is the Drude scattering time. Therefore, our experimental approach of monitoring changes in the peak amplitude of the transmitted THz pulse is valid [36].

Figure 2(b) shows the negative change in transmission ($-\Delta T$) of the peak of the THz pulse as a function of delay time at 10 K. The rise time of the signal is limited by the 0.5 ps response time of the THz pulse setup [36]. The signal decays quickly over the first few picoseconds and then more slowly at longer times. Similar dynamics,

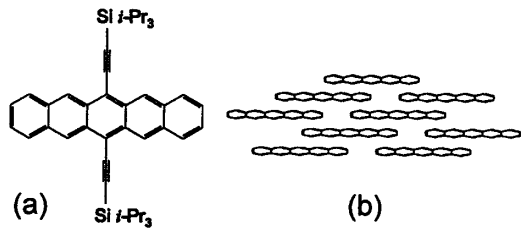

FIG. 1. (a) Molecular structure of FPc. (b) Stacking of FPC in the *a-b* plane of crystal (side groups not shown).

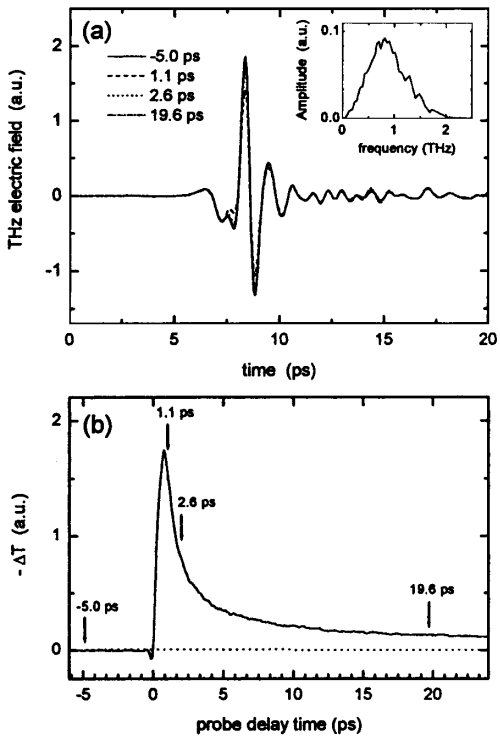

FIG. 2. (a) THz pulses transmitted through a FPc crystal at 10 K at various probe delay times. The 800 nm, 100 fs pump pulse excites the sample at $t = 0$, and the probe delay time is the arrival time of the positive peak of the THz probe pulse. The inset shows the amplitude spectrum of the THz probe pulse transmitted through the unexcited sample. (b) Change in amplitude transmission of the peak of the THz probe pulse as a function of delay time at 10 K. (Pump fluence is 2.5 mJ/cm^2.)

but much smaller signals, are observed at room temperature. Pump-induced thermal transients in the sample are less than 1 K, which is too small to explain the observed changes in transmission. Heat and carrier diffusion times out of the excitation volume are much too long ($\sim 10^{-3}$ s) to account for the observed sub-ns response. Two-photon absorption does not contribute significantly to carrier generation since the change in transmission of the THz pulse is nearly linear with pump intensity.

Differential transmission is defined as $\Delta T/T_0 = (T - T_0)/T_0$, where T_0 is the transmission of the THz pulse through the unexcited sample. It can be shown that if $|\Delta T/T_0| < 20\%$, then $-\Delta T/T_0$ is approximately proportional to the conductivity $\sigma = ne\mu$, where n is the carrier density, e is the electronic charge, and μ is the effective mobility of the carriers [36]. The temperature dependence of the percent differential transmission of the THz pulse through sample A is shown in Fig. 3(a). Note that the signals get larger as the temperature is lowered. Similar behavior was observed for sample B. The 0.5 ps rise time of the photoconductivity transients is shown in the inset of Fig. 3(a). Figure 3(b) is a log-log plot of the data shown in Fig. 3(a). The exact dynamics of the fast initial decay for the first 2 ps is difficult to resolve due to the time resolution of the experimental setup [42]. At longer times, however, a power-law decay is observed.

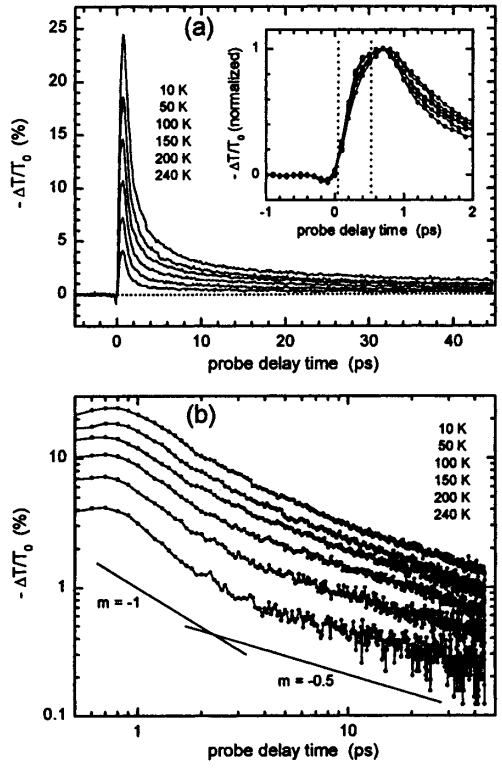

FIG. 3. (a) Percent differential transmission of the peak of the THz probe pulse as a function of delay time and temperature for sample A. The photoconductivity transients increase as the temperature decreases. The inset shows a 10%–90% rise time of 0.5 ps for the transients. (b) Log-log plot of the data shown in (a). Lines labeled $m = -1$ and $m = -0.5$ are guides to the eye for power-law decay rates of t^{-1} and $t^{-0.5}$, respectively. (Pump fluence is 2.5 mJ/cm^2.)

The increase in the peak of the transient signal as the temperature is lowered is shown in Fig. 4(a). We attribute this behavior to an increase in carrier mobility at low temperatures (assuming the initial density of photoexcited carriers is independent of temperature). At 10 K, $|\Delta T/T_0|_{\max} \cong 24\%$, which corresponds to an initial carrier mobility of about 1.6 cm^2/V s for an injected carrier density of 7.5×10^{17} cm^{-3} [36]. This is a lower estimate since it assumes 100% internal quantum efficiency for the generation of free carriers, which may not be valid due to geminate recombination, and it also neglects the finite response time of the setup, which makes the measured $|\Delta T/T_0|_{\max}$ smaller than the true value. The mobility scales with $|\Delta T/T_0|_{\max}$ as a function of temperature, giving room temperature values of about 0.2 cm^2/V s. This is comparable to earlier estimates of about 1 cm^2/V s for FPc crystals at room temperature [40]. (Note that if we assume a quantum efficiency of only 10% in FPc, then the estimated transient mobilities at 10 K and 300 K increase to 16 cm^2/V s and 2 cm^2/V s, respectively.) While the mobility values for these crystals are still orders of magnitude less than low-temperature values reported elsewhere for ultrapure Pc [17], they are surprisingly high for simple solution-grown crystals that likely contain significant defect sites.

We attribute the power-law decay, $-\Delta T/T_0 \sim t^{-\beta}$, at times longer than 4 ps [Fig. 3(b)] to dispersive transport. The temperature dependence of the exponent β is shown in Fig. 4(b). If $t^{-\beta} = t^{\alpha-1}$, where α is the dispersion parameter mentioned earlier, then $\beta = 1 - \alpha$. In multiple trapping models, $\alpha = T/T_0$, where T_0 is a characteristic temperature, and μ decreases as the temperature is lowered [14,43]. This is incompatible with our results that

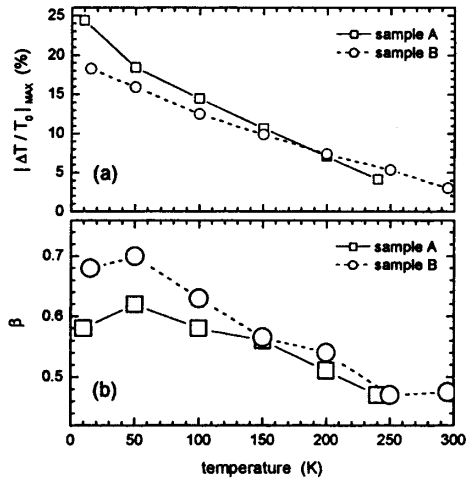

FIG. 4. Temperature dependence of (a) the peak differential transmission and (b) the exponent β for a power-law fit $t^{-\beta}$ at long times for sample A (squares) and sample B (circles). The error bars are smaller than the size of the symbols.

show a nearly temperature independent β that does not approach unity at low temperatures and a mobility that increases as the temperature decreases. However, dispersive transport with temperature independent exponents has been reported in polyvinylcarbazole [12], polyacetylene [44], and C_{60} thin films [45], and has been attributed to intermolecular hopping processes [45] and nonactivated tunneling between sites with equivalent energies [15]. It is interesting to note that the nearly small molecular polaron model proposed by Silinsh *et al.* [8] uses nonactivated tunneling to describe bandlike transport of polarons in polyacene crystals.

Finally, since THz pulses detect the presence of free carriers, the rapid rise of $-\Delta T/T_0$ to its maximum value at 0.7 ps (Fig. 3) suggests that free carriers (i.e., polarons) are primary photoexcitations in FPc. As shown in the inset of Fig. 3(a), the 10%–90% rise time of the transients is 0.5 ps, which is equivalent to the minimum response time of our THz pulse setup. Therefore, we expect the formation of mobile carriers in FPc crystals to occur over time scales much shorter than 0.5 ps. For comparison, the formation of polarons in 100 fs has been observed in polymer thin films [24,25], whereas electric-field-assisted dissociation of excitons into polarons in about 10 ps has been reported [23]. We found that the amplitude of the electric field of the THz probe pulse did not affect the magnitude of our $\Delta T/T_0$ signals, thereby eliminating THz-field-induced dissociation of excitons as a possible carrier generation mechanism in our experiments. (The peak electric field of the THz pulse at the sample was less than 10^3 V/cm.) Perhaps the initial fast decay is a result of bandlike transport of photoexcited carriers that couple to the lattice and form polarons [46] over time scales of 1–2 ps. On the other hand, trap filling effects may also play a role. To address these possibilities, more experiments with purer crystals will be necessary.

In conclusion, we have measured the transient photoconductivity in molecular crystals of functionalized pentacene using terahertz pulse techniques. The rapid onset of photoconductivity suggests that mobile carriers are a primary photoexcitation in these crystals. Transient mobilities of at least 1.6 $cm^2/V\,s$ at 10 K were obtained, and dispersive transport at long times was observed.

We thank A. D. Slepkov, D. Mullin, R. McDonald, and Y. Zhao for assistance. We acknowledge useful discussions with J. S. Brooks and F. Marsiglio, and support from NSERC, CFI, IIPP, ASRA, CIPI, and ONR.

*Electronic address: hegmann@phys.ualberta.ca

[1] M. R. Baldo *et al.*, Nature (London) **403**, 750 (2000).
[2] H. Klauk *et al.*, IEEE Electron Device Lett. **20**, 289 (1999).
[3] V. G. Kozlov *et al.*, Nature (London) **389**, 362 (1997).
[4] J. H. Schön *et al.*, Nature (London) **403**, 408 (2000).
[5] N. S. Sariciftci, *Primary Photoexcitations in Conjugated Polymers: Molecular Exciton versus Semiconductor Band Model* (World Scientific, Singapore, 1997).
[6] M. Pope and C. E. Swenberg, *Electron Processes in Organic Crystals* (Clarendon, Oxford, 1982).
[7] E. A. Silinsh and V. Cápek, *Organic Molecular Crystals: Interaction, Localization, and Transport Phenomena* (American Institute of Physics, New York, 1994).
[8] E. A. Silinsh *et al.*, Chem. Phys. **198**, 311 (1995).
[9] A. J. Heeger, Rev. Mod. Phys. **73**, 681 (2000).
[10] A. B. Kaiser, Rep. Prog. Phys. **64**, 1 (2001).
[11] J. L. Brédas and G. B. Street, Acc. Chem. Res. **18**, 309 (1985).
[12] F. C. Bos and D. M. Burland, Phys. Rev. Lett. **58**, 152 (1987).
[13] D. Hertel *et al.*, J. Chem. Phys. **110**, 9214 (1999).
[14] T. Tiedje, in *Semiconductors and Semimetals*, edited by J. I. Pankove (Academic Press, Orlando, 1984), Vol. 21, Pt. C, p. 207.
[15] H. Scher and E.W. Montroll, Phys. Rev. B **12**, 2455 (1975); H. Scher *et al.*, Phys. Today **44**, No. 1, 26 (1991).
[16] W. Warta and N. Karl, Phys. Rev. B **32**, 1172 (1985).
[17] J. H. Schön *et al.*, Phys. Rev. B **63**, 245201 (2001).
[18] *Semiconductors—Basic Data*, edited by O. Madelung (Springer-Verlag, Berlin, 1996).
[19] L. B. Schein *et al.*, Phys. Rev. Lett. **40**, 197 (1978).
[20] J. H. Schön *et al.*, Phys. Rev. Lett. **86**, 3843 (2001).
[21] V. M. Kenkre and P. E. Parris, Phys. Rev. B **65**, 205104 (2002).
[22] R. Kersting *et al.*, Phys. Rev. Lett. **73**, 1440 (1994).
[23] W. Graupner *et al.*, Phys. Rev. Lett. **81**, 3259 (1998).
[24] P. B. Miranda *et al.*, Phys. Rev. B **64**, 08120(R) (2001).
[25] D. Moses *et al.*, Phys. Rev. B **61**, 9373 (2000).
[26] S. V. Frolov *et al.*, Phys. Rev. B **63**, 205203 (2001).
[27] S. V. Frolov *et al.*, Chem. Phys. Lett. **334**, 65 (2001).
[28] D. Moses *et al.*, Phys. Rev. B **59**, 7715 (1999).
[29] T.-I. Jeon and D. Grischkowsky, Phys. Rev. Lett. **78**, 1106 (1997).
[30] J. S. Dodge *et al.*, Phys. Rev. Lett. **85**, 4932 (2000).
[31] R. A. Kaindl *et al.*, Phys. Rev. Lett. **88**, 027003 (2002).
[32] T.-I. Jeon *et al.*, Appl. Phys. Lett. **79**, 4142 (2001).
[33] M. Schall and P. Uhd Jepsen, Opt. Lett. **25**, 13 (2000).
[34] M. C. Beard *et al.*, Phys. Rev. B **62**, 15 764 (2000).
[35] S. S. Prabhu *et al.*, Appl. Phys. Lett. **70**, 2419 (1997).
[36] K. P. H. Lui and F. A. Hegmann, Appl. Phys. Lett. **78**, 3478 (2001); F. A. Hegmann and K. P. H. Lui, Proc. SPIE-Int. Soc. Opt. Eng. **4643**, 31 (2002).
[37] R. D. Averitt *et al.*, Phys. Rev. Lett. **87**, 017401 (2001).
[38] E. Knoesel *et al.*, Phys. Rev. Lett. **86**, 340 (2001).
[39] M. C. Beard *et al.*, J. Chem. Phys. A **106**, 878 (2002).
[40] J. E. Anthony *et al.*, J. Am. Chem. Soc. **123**, 9482 (2001); J. S. Brooks *et al.*, Curr. Appl. Phys. **1**, 301 (2001).
[41] T. Tokumoto *et al.*, J. Appl. Phys. **92**, 5208 (2002).
[42] Deconvolution techniques will be presented elsewhere.
[43] J. Orenstein and M. A. Kastner, Solid State Commun. **40**, 85 (1981).
[44] S. Etemad *et al.*, Solid State Commun. **40**, 75 (1981).
[45] R. Könenkamp *et al.*, Phys. Rev. B **60**, 11 804 (1999).
[46] D. Emin and A. M. Kriman, Phys. Rev. B **34**, 7278 (1986).